HHS Public Access

Author manuscript

Leukemia. Author manuscript; available in PMC 2016 May 18.

Published in final edited form as:

Leukemia. 2016 March ; 30(3): 617–626. doi:10.1038/leu.2015.302.

A phosphodiesterase 4B-dependent interplay between tumor cells and the microenvironment regulates angiogenesis in B-cell lymphoma

Avvaru N. Suhasini[1], **Long Wang**[#1], **Kenneth N. Holder**[#2], **An-Ping Lin**[1], **Harshita Bhatnagar**[1], **Sang-Woo Kim**[1,#], **August W. Moritz**[2], and **Ricardo C. T. Aguiar**[1,3,4]

[1]Division of Hematology and Medical Oncology, Department of Medicine, University of Texas Health Science Center at San Antonio.

[2]Department of Pathology, University of Texas Health Science Center at San Antonio

[3]Greehey Children's Cancer Research Institute, University of Texas Health Sciences Center at San Antonio.

[4]South Texas Veterans Health Care System, Audie Murphy VA Hospital, San Antonio.

[#] These authors contributed equally to this work.

Abstract

Angiogenesis associates with poor outcome in diffuse large B-cell lymphoma (DLBCL), but the contribution of the lymphoma cells to this process remains unclear. Addressing this knowledge gap may uncover unsuspecting proangiogenic signaling nodes and highlight alternative antiangiogenic therapies. Here we identify the second messenger cyclic-AMP (cAMP) and the enzyme that terminates its activity, phosphodiesterase 4B (PDE4B), as regulators of B-cell lymphoma angiogenesis. We first show that cAMP, in a PDE4B-dependent manner, suppresses PI3K/AKT signals to down-modulate VEGF secretion and vessel formation in vitro. Next, we create a novel mouse model that combines the lymphomagenic Myc transgene with germline deletion of *Pde4b*. We show that lymphomas developing in a *Pde4b*-null background display significantly lower microvessel density in association with lower VEGF levels and PI3K/AKT activity. We recapitulate these observations by treating lymphoma-bearing mice with the FDA-approved PDE4 inhibitor Roflumilast. Lastly, we show that primary human DLBCLs with high PDE4B expression display significantly higher microvessel density. Here, we defined an

Correspondence to: Ricardo Aguiar, MD PhD, Department of Medicine, University of Texas Health Science Center at San Antonio, 7703 Floyd Curl Drive, San Antonio, TX, 78229, Phone: 1-210-567-4860, ; Email: aguiarr@uthscsa.edu

[#]current address: Department of Biological Sciences, Pusan National University, 63 Beon-gil 2, Busandaehag-ro, Geumjeong-gu, Pusan 609–735, Republic of Korea

Supplementary information is available at Leukemia's website

Author Contributions: Author Contributions: A.N.S, designed and conducted experiments, and analyzed the data; L.W. conducted animal experiments; A-P.L conducted experiments, H.B. performed animal husbandry; S-W Kim conducted experiments; AM and K.H performed pathological analyses; R.C.T.A designed and coordinated the study, analyzed data and wrote the manuscript, which was reviewed by all authors.

Conflict of interest: The authors have no conflict of interest to disclose

unsuspected signaling circuitry in which the cAMP generated in lymphoma cells downmodulates PI3K/AKT and VEGF secretion to negatively influence vessel development in the microenvironment. These data identify PDE4 as an actionable antiangiogenic target in DLBCL.

Introduction

Angiogenesis, the development of new blood vessels from preexisting vasculature, results from the production of proangiogenic factors by cancer and non-malignant cells in the tumor microenvironment[1]. This abnormal vascular network is critical for the tumor metabolism and for its metastatic potential[2]. Thus, the concept of targeting the tumor blood supply, primarily with agents that directly inhibit vascular endothelial growth factor (VEGF) signals, has been incorporated in cancer treatment[1, 2]. These antiangiogenic strategies have improved clinical response in some settings, but the benefits are often modest and of limited impact on overall survival[1, 2].

Diffuse Large B-cell lymphoma (DLBCL) is a heterogeneous malignancy derived from mature B-cells[3]. Examination of the transcriptional and genetic landscape of DLBCL identified gene signatures associated with outcome and mechanisms of transformation[4-6], and uncovered the contribution of chromatin regulators to the disease biology[7]. However, this knowledge has yet to be translated into effective rationally-developed treatment strategies, and first-line immunochemotherapy (R-CHOP) remains curative for only about 60% of the DLBCL patients[3]. Recognizing and acquiring basic biology data in specific priority areas may accelerate clinical translation in DLBCL[8]. One such knowledge gap concerns the interplay between lymphoma cells, the microenvironment and angiogenesis. Addressing this problem is particularly important because high circulating levels of VEGF and increased microvessel density in the lymphoma microenvironment are associated with poor outcome in DLBCL[5, 9-12]. Unfortunately, the combination of anti-VEGFA agents with R-CHOP was associated with prohibitive cardiotoxicity and did not improve survival[13, 14]. Thus, a better understanding of the contribution of the lymphoma cell to angiogenesis also has the potential to identify alternative antiangiogenic therapeutic strategies in DLBCL.

Cyclic-AMP (cAMP) is a pervasive second messenger that in immune cells exerts predominantly negative effects, including suppression of B or T cell receptor signaling, modulation of cytokine production and apoptosis[15-19]. Intra-cellular cAMP signaling is terminated by phosphodiesterases and in immune cells the phosphodiesterase 4 (PDE4) family catalyze most of the cAMP hydrolysis[20]. Earlier, we identified PDE4B overexpression in an outcome prediction signature in DLBCL[21]. Subsequently, we showed that PDE4B contributes to DLBCL aggressiveness by abrogating the cAMP-mediated inhibition of PI3K/AKT and SYK signaling[17, 18, 22]. The consequences of cAMP activity are highly contextualized and cell type specific[19, 20]. Thus, it is of interest that cAMP has been shown to attenuate vessel development in non-neoplastic cell models, at least in part by acting on endothelial cells[23-26]. However, whether cAMP can influence the secretion of proangiogenic factors by lymphoma cells and thus modulate the cross talk between tumor and microenvironment remains to be determined.

To examine this possibility, we developed in vitro systems, generated a novel mouse and examined primary DLBCL samples. In DLBCL cell lines, we show that cAMP down-modulates VEGF transcription/secretion and vessel formation in a PDE4B-dependent manner. DLBCL cell lines expressing high levels of PDE4B have a proangiogenic profile that can be suppressed by genetically or pharmacologically inhibiting PDE4. Mechanistically, we show that the cAMP-PDE4B axis impinges on VEGF by modulating PI3K and AKT signals. We also created a mouse model where c-Myc-driven lymphoma develops in a *Pde4b−/−* background. Remarkably, Pde4-null B-cell lymphomas displayed significantly suppressed angiogenesis, an effect that could be recapitulated by treating Pde4b-competent murine B-cell lymphoma with the FDA approved PDE4 inhibitor Roflumilast. Examination of the B-cell lymphomas harvested from these in vivo models confirmed that PDE4B influences VEGF levels via the PI3K/AKT pathway. Lastly, we showed that PDE4B expression positively correlates with angiogenesis in primary DLBCL biopsies. Together, these data uncovered a previously unappreciated cAMP-mediated signaling cross-talk between the lymphoma cells and the microenvironment that regulates angiogenesis in vivo, and point to PDE4 inhibition as an antiangiogenic therapeutic strategy for DLBCL and related mature B-cell tumors.

Materials and Methods

(see supplementary data for detailed methodology)

Cell lines and primary DLBCL

DLBCL cell lines (SU-DHL4, SU-DHL6, SU-DHL10, OCI-Ly4, OCI-Ly10 and OCI-Ly18) were cultured as we described[27]. Paired paraffin blocks and RNA were available from 28 untreated DLBCL patients. The use of these anonymized samples was approved by the Institutional Review Board of the UT Health Science Center San Antonio (UTHSCSA).

Mice

To generate the compound *Pde4b−/−; Eμ-Myc-Tg* mice, *Pde4b+/−* females[28] were bred to *Eμ-Myc-Tg* males. Subsequently, *Pde4b+/−* females were crossed to *Pde4b+/−;MycTg* males, creating the desired *Pde4b−/−;Eμ-Myc-Tg* strain and control *Pde4b+/+;Eμ-Myc-Tg* mice. For the adoptive transfer assays, C57BL/6 mice were transplanted with *Eμ-Myc-Tg*-derived lymphoma cells and randomized to receive the PDE4 inhibitor Roflumilast or control. All procedures were approved by the IACUC of the UTHSCSA.

VEGF and cAMP quantification

VEGFA abundance was examined at RNA and protein levels, in human and murine samples, using real-time RT-PCR[29] and the Human or Mouse VEGF Immunoassay (R&D Systems), respectively. Intra and extracellular (conditioned media) cAMP levels were measured using ELISA (Parameter cAMP assay; R&D Systems).

Tube formation assay

Performed on low passage sub-confluent human umbilical vein endothelial cells (HUVEC, Life Technologies) using conditioned media from DLBCL cell lines.

PI3K assay

Quantification of PI3K activity was performed on whole-cell lysates collected from DLBCL cell lines or primary murine lymphomas, utilizing an ELISA-based assay (Echelon Biosciences).

Genetic models and western blots

DLBCL cell lines stably expressing PDE4B and AKT constructs, or with siRNA-mediated PDE4B KD were described earlier[17, 18, 22]. Western blots for PDE4B, AKT, FLAG and Actin were performed as we described[30].

Histopathology

Slides stained for CD34 were digitally scanned and examined in a blinded fashion for microvessel density (MVD) quantification using Aperio ImageScope software (Leica Biosystems). For each case, 3 hot spots (area of maximal MVD) were examined and all microvessels manually counted and highlighted using the ImageScope software, which calculated the area of each vessel.

Statistics

Analyses performed with GraphPad Prism5 software included two-tailed Student's t test, one-way analysis of variance (ANOVA), Spearman's rank correlation coefficient, and log-rank test. $P < 0.05$ was considered significant.

Results

cAMP/PDE4B-mediated modulation of VEGFA in DLBCL

Using a panel of DLBCL cell lines dichotomized by *PDE4B* expression/activity (Supplementary Figure 1), we investigated whether the cAMP-PDE4B axis influenced VEGFA levels. Increasing intra-cellular cAMP (via pharmacologic activation of adenylyl cyclases with Forskolin) suppressed *VEGFA* mRNA levels in *PDE4B*-low but not *PDE4B*-high cells (Figure 1A). In agreement with the mRNA data, cAMP inhibited VEGF secretion in the conditioned media of the DLBCL cell lines in a PDE4B-dependent manner (Figure 1B). The cAMP analog 8-Br-cAMP confirmed that the suppression of VEGF in DLBCL cell lines exposed to Forskolin derived from elevation of cAMP levels (Supplementary Figure 2). Using HUVEC tube formation assays, we show that cAMP inhibited vessel formation capability of conditioned media from PDE4B-low, but not PDE4B-high DLBCL cells (Figure 1C). Importantly, because cAMP can directly inhibit endothelial cells[25, 26], we established several safeguards to guarantee that the HUVEC assays are reflective of the effects of cAMP on the production of VEGF by the lymphoma cells, and not from a fortuitous presence of Forskolin and/or cAMP in the conditioned media (see Supplemental Methods, Supplementary Figure 3). We concluded that in DLBCL cell lines cAMP suppresses VEGF levels and in vitro vessel development in a PDE4B-dependent manner.

Genetic and pharmacological approaches confirm the role of PDE4B in regulating cAMP-mediated VEGF suppression

To isolate the role of PDE4B in the cAMP/VEGF interplay, we used genetic and pharmacological approaches. First, we stably expressed PDE4B wild-type (WT) or phosphodiesterase inactive mutant genes in a PDE4B-low DLBCL cell line. Expression of WT PDE4B abrogated the suppressive effects of cAMP on VEGF secretion and HUVEC tube formation whereas the mutant phosphodiesterase was as ineffective as the empty vector (Figure 2A). Using a siRNA strategy in a PDE4B-high cell line, we showed that PDE4B knockdown significantly suppressed VEGF secretion and tube formation (Figure 2B, Supplementary Figure 4). Lastly, in multiple PDE4B-high DLBCLs, exposure to the PDE4 inhibitor Roflumilast resulted in a significant decrease in VEGF secretion, which was accompanied by reduced tube formation capacity (Figure 2C). We concluded that PDE4B regulates cAMP-mediated suppression of VEGF in DLBCL, suggesting that the levels/activity of PDE4B in lymphoma cells may influence angiogenesis in the tumor microenvironment.

The PDE4B-cAMP axis influences VEGF expression by modulating PI3K/AKT signals

We investigated if the cAMP-mediated/PDE4B-dependent modulation of VEGF expression in DLBCL was related to the suppression of PI3K/AKT that we reported earlier[18]. Cyclic-AMP significantly suppressed PI3K activity in PDE4B-low but not in PDE4B-high DLBCL cell lines (Figure 3A). Further, ectopic expression of WT PDE4B, but not the inactive enzyme, blocked cAMP suppression of PI3K (Figure 3B). AKT plays a crucial role in the regulation of VEGF under normoxic conditions[31]. Thus, we reasoned that downstream to PI3K, cAMP/PDE4B uses AKT to regulate VEGF. Indeed, phosphorylation of AKT's threonine 308 was markedly suppressed by cAMP in the cells expressing low, but not high PDE4B levels and rescued by the WT but not the inactive enzyme (Figure 3C). Lastly, we expressed a myristoylated form of AKT in PDE4B-low cells and re-examined the effects of cAMP on PI3K activity, VEGF secretion and tube formation. As PI3K is upstream to AKT, even in the context of a constitutively active AKT, cAMP readily suppressed this lipid kinase activity (Figure 3D). However, in these cells cAMP did not suppress AKT, VEGF secretion and the development of vessel like structures (Figure 3D). We concluded that in DLBCL cell lines cAMP-PDE4B modulates VEGF and angiogenesis via the PI3K/AKT pathway.

Genetic deletion of *Pde4b* limits angiogenesis in vivo

To advance the concept that PDE4B controls angiogenesis in B-cell lymphoma, we generated a novel compound mouse that combines the lymphomagenic Myc transgene with homozygous deletion of the *Pde4b* gene *(Pde4b−/−;Eμ-Myc-Tg*). Although the *Eμ-Myc* mice develop B-cell lymphomas with variable degrees of maturation[32], its dependence on c-myc and on secondary hits on p53 and BCL-2, recapitulates in part the biology of mature B-cell lymphomas[33]. For these reasons, as well as its high penetrance and short latency, this mouse has been instrumental in the identification of lymphomagenic processes and response to targeted agents[34–38]. The *Pde4b−/−;Eμ-Myc-Tg* mice and their *Pde4b+/+;Eμ-Myc-Tg* counterparts were followed clinically for evidence of lymphoma (see Supplementary Table 1 for features of lymphomas developed in *Pde4b*+/+ or *Pde4b*−/− mice). Upon tumor

diagnosis, the mice (n=19) were sacrificed and lymphomas collected for histological characterization and IHC-based quantification of angiogenesis with anti-CD34 staining. Remarkably, lymphomas that developed in a *Pde4b*-null background displayed significantly lower microvessel density (Figure 4A). In addition, *Pde4b*−/− primary lymphomas showed lower PI3K activity, phospho-AKT levels (Figure 4B), and VEGF expression than tumors that developed in the *Pde4b*-WT mice (Figure 4C). We concluded that the Pde4b/Pi3k/Akt/Vegf axis is active in vivo, that the genetic deletion of *Pde4b* suppresses VEGF expression in the tumor cells and inhibit angiogenesis in the microenvironment of primary murine B-cell lymphomas.

Pharmacological targeting of Pde4 limits angiogenesis and improves survival in a murine model of B-cell lymphoma

The data obtained in the mice described above were very informative and reinforced the concept that Pde4b expression modulates angiogenesis in B-cell lymphomas. However, in this model *Pde4b* is deleted in the germline, thus not fully recapitulating the clinical use of PDE4 inhibitors. To address this concern, we used adoptive transfer and treated lymphoma-harboring mice with the PDE4 inhibitor Roflumilast. We generated four independent mouse cohorts (n=68), each derived from a unique *Eμ-Myc-Tg* B-cell lymphoma. In the first two groups (n=16), tumors developed at day 10 post-transplant and the mice were randomized to receive Roflumilast (5mg/kg/day by gavage) or vehicle control; after five days of treatment all mice were sacrificed and tumors collected for MVD quantification. Lymphomas from Roflumilast-treated mice displayed a significantly lower vessel density than tumors that developed in vehicle-treated mice (Figure 5A). To link the antiangiogenic effects of PDE4 inhibition to the suppression of VEGF, we transplanted a third cohort of mice (n=8), randomized them into Roflumilast or vehicle control. This time, in addition to lymph nodes for histopathology and IHC, we also collected sera for VEGF quantification. We confirmed that Roflumilast treatment significantly decreased MVD and showed that this effect was associated with significantly lower levels of circulating VEGF (Figure 5B). In these three independent cohorts (n=24 mice), the lymphomas displayed an aggressive behavior and since we waited until day 10 post-transplant to randomize the mice, they were uniformly sacrificed with progressive disease 5 days into treatment. To address the limitations associated with this short clinical follow up, we tested dosing Roflumilast on day 5 post-transplant, before clinical evidence of lymphoma. In a pilot assay (n=8), mice receiving prophylactic Roflumilast had a significant decrease in lymphoma-associated MVD and circulating VEGF (Supplementary Figure 5), and also a modest improvement in survival. We then designed an experiment with enough power to test the hypothesis that in association with suppression of angiogenesis, Pde4 inhibition may limit lymphoma growth and improve survival. We transplanted a cohort of 36 mice and randomized them on day 5 into vehicle or Roflumilast groups; mice were followed clinically and sacrificed when there was evidence of widespread disease or at treatment day 30, whichever came first. At the completion of the experiment, the median survival of the Roflumilast treated mice had not yet been reached and it was 23 days for the vehicle treated group (p=0.01, log-rank test); 10 mice in the Roflumilast group and 2 in vehicle-treated were alive at the time the assay was terminated (Figure 5C). Further, lymphomas that arose in the Roflumilast-treated mice were significantly smaller than the isogenic tumors that developed in the control group (Figure

5C), and displayed significantly lower PI3K activity, AKT phosphorylation and VEGF levels than the control group (Figure 5D). We concluded that pharmacological inhibition of PDE4 suppresses lymphoma angiogenesis in vivo, in association with reduced PI3K/AKT activity and VEGF levels. This profile is accompanied by a decreased tumor burden and improved survival, suggesting that PDE4 inhibitors have anti-lymphoma activity.

PDE4B expression correlates with angiogenesis in primary human DLBCL

To further define the relevance of our in vitro and in vivo data, we tested whether *PDE4B* expression correlates with angiogenesis in primary human DLBCLs. Paired paraffin blocks and RNA were available from 28 untreated DLBCL cases[39, 40]. Anti-CD34 staining was used to identify the MVD in these primary DLBCL and Q-RT-PCR employed for quantification of *PDE4B* expression. The latter was selected as the approach of choice since multiple attempts to establish IHC staining for PDE4B with available antibodies were unsuccessful, and good quality protein from these specimens were not available for western blot-based examinations. Importantly, as we showed before[18] (and in Supplementary Figure 1) there is a very good correlation between PDE4B mRNA and protein expression indicating that this Q-RT-PCR assay captures relevant information. First, in agreement with earlier observations[5, 11, 12, 41, 42], we found a significant variability in the degree of angiogenesis in the microenvironment of DLBCLs. Likewise, as we defined earlier[18], there was a broad range of PDE4B expression across the DLBCL biopsies (Supplementary Figure 6). Remarkably, we detected a significant direct correlation between *PDE4B* levels and MVD in DLBCL (r=0.43, p=0.02) (Figure 6). These data are particularly relevant for they derive from unmodified and heterogeneous primary human tumors, in which a given phenotype (e.g. angiogenesis) is likely to be influenced by multiple genetic inputs. Together, these observations agree with our in vitro and mouse model data, and suggest that PDE4B expression may contribute to angiogenesis in human DLBCL.

Discussion

Exacerbated angiogenesis associates with poor outcome in DLBCL[5, 9, 11, 14]. However, little is known about the contribution of the lymphoma cells to this process. Here, we detail a novel role for the second messenger cAMP and the enzyme PDE4B in regulating new vessel development in B-cell lymphoma. Further, using a FDA-approved PDE4 inhibitor we demonstrate the immediate translational potential of this discovery.

The interplay between lymphoma cells, the microenvironment and angiogenesis remains poorly understood[5, 11]. Our data show that the expression and activity of PDE4B in DLBCL cell lines and in primary murine B-cell lymphomas regulate VEGF secretion in the microenvironment and angiogenesis. The identification of PDE4B overexpression in a gene signature associated with poor outcome in DLBCL established the first link between this enzyme and B-cell lymphomas[21]. Subsequently, we showed that in normal and malignant mature B-cells, cAMP markedly suppresses the activity of kinases related to proximal B-cell receptor (BCR), in particular SYK and PI3K[17, 18]. As phosphodiesterases hydrolyze cAMP, DLBCL cells with elevated PDE4B expression display heightened SYK and PI3K activity, which may in part explain how it could influence lymphoma aggressiveness. The data that

we report now establish angiogenesis as a novel paradigm for PDE4B contribution to an adverse outcome in DLBCL. Notably, despite some discordant reporting, the role of angiogenesis to DLBCL outcome appears to be independent from the germinal center B-cell (GCB) and activated B-cell-like (ABC) dichotomy[5, 11, 41]. Similarly, the expression of PDE4B in primary DLBCL and DLBCL cell lines is independent of the cell-of-origin classifier[6, 17, 18].

We expanded on our in vitro observations, by creating an mouse that combines a lymphoma-driving allele (*Eμ-Myc*) with homozygous deletion of *Pde4b*. B-cell lymphomas that developed in these mice showed significantly diminished angiogenesis. PDE4 is an actionable target and we recapitulated the effects of the genetic deletion of *Pde4b* on angiogenesis by treating mice harboring B-cell lymphomas with Roflumilast. These observations are relevant at several levels. First, with the recognized role of VEGF/angiogenesis in DLBCL outcome[9-11], but the prohibitive toxicity of bevacizumab in DLBCL patients[13, 14], Roflumilast presents an attractive, biologically sound, therapeutic strategy to inhibit lymphoma angiogenesis. Second, because Roflumilast is FDA approved its effects on DLBCL angiogenesis in humans can be promptly tested. Of note, we recently activated a small Phase 0/I trial of Roflumilast in patients with advanced mature B-cell malignancies (clinical trial# NCT01888952) and the results of this trial will be relevant in designing new trials centered on antiangiogenesis. Third, although we clearly isolated the contribution of PDE4B to B-cell lymphoma angiogenesis, other members of the PDE4 family, notably PDE4D, are also expressed in lymphocytes[43]. Thus, the use of pan-PDE4 inhibitor such as Roflumilast may actually be beneficial in this setting. Lastly, although the outcome of cAMP signaling and the pattern of phosphodiesterase expression are tissue specific, it will be important to define in future studies whether PDE4 inhibition also downmodulates angiogenesis in malignancies other than lymphomas. The suggestions that PDE4 targeting may have a place in the treatment of highly vascularized brain tumors and colon cancer[44, 45] provide rationale for implementing these investigations.

Cyclic-AMP is also known to negatively influence the ability of endothelial cells to migrate, adhere and survive during angiogenesis[25, 26]. Thus, it is possible that in the mouse model that we created, the constitutive homozygous deletion of *Pde4b* inhibits angiogenesis both via the suppression of VEGF secretion by the lymphomas cells and perhaps also by directly impacting on the endothelial cells. While this may occur in this model, our data demonstrate an unequivocal contribution of lymphoma cells in the control of angiogenesis. In brief, using IHC staining of murine B-cell lymphomas, we identified the tumor cells as the main source of VEGF, and demonstrate that its expression is suppressed in the lymphoma developing in a Pde4b-null background. Also, in in vitro models, where DLBCL are cultured in absence of endothelial cells, we demonstrated that the cAMP-mediated/PDE4B-dependent decrease in VEGF secretion limits the subsequent formation of vessel like structures by HUVECs. Importantly, we recapitulated the suppression of lymphoma angiogenesis detected in the genetically engineered Pde4b-null mouse with Roflumilast in vivo. Thus, employing a pharmacological approach that closely approximates a clinical initiative in humans we effectively suppressed lymphoma angiogenesis. For these reasons, the precise mapping of the relative contribution of PDE4 inhibition on lymphoma versus endothelial cells becomes, at this juncture, less critical. We suggest that effectiveness of Roflumilast in our in vivo

model mitigates concerns that the constitutive deletion of *Pde4b* in the mice germline had other unappreciated effects that significantly contributed to the suppression of B-cell lymphoma angiogenesis.

Curiously, whereas treatment with Roflumilast and the knockout of the *Pde4b* gene in the mouse germline equally inhibited lymphoma angiogenesis, only the former modified the natural history of the Myc-driven B-cell lymphomas. In fact, although Roflumilast-treated mice had lower tumor burden and lived longer, the survival of Eμ-Myc mice was similar irrespective of *Pde4b* status (Supplementary Table 1). The precise reasons for these discrepancies are not immediately clear, but a few possibilities exist. In addition to its role in lymphoma and endothelial cell biology, as discussed above, Pde4b inhibition also suppresses the inflammatory response, as well as several aspects of the innate and acquired immune response[15, 16, 28, 46]. Thus, it could be speculated that deletion of this gene in the germline constitutively limits the activity of multiple cellular components involved in tumor surveillance, which in a pro-oncogenic context (e.g. Eμ-myc transgene) may contribute to tumor emergence and maintenance. Alternatively, the improved survival of mice harboring Myc-driven B-cell lymphomas treated with Roflumilast may relate to its ability to inhibit not only PDE4B but also the other members of the PDE4 family of phosphodiesterases, as we highlighted above. Irrespective of the reason(s) for the discrepancy between the genetic and pharmacological models that we explored in this work, these results should be viewed with the realization that it is the successful pharmacological inhibition of PDE4, which we achieve in the preclinical murine models, not the genetic modulation of PDE4B levels that will be translated into clinic initiatives. In future work, the generation of mouse models with conditional deletion of Pde4b and/or other Pde4 genes in mature B-cells, alongside the use lymphomagenic drivers other than Myc, should help parse out the relative contribution of depleting individual PDE4 genes in different cell types on lymphoma development and progression.

Mechanistically, our data implicated the PI3K/AKT pathway as mediator of the cAMP-PDE4B effects on VEGF. These observations uncovered an additional paradigm for how cAMP may attenuate vessel development in non-neoplastic and neoplastic tissues[23–26, 47]. Perhaps more importantly, uncovering the participation of PI3K/AKT on the PDE4B-mediated regulation of lymphoma angiogenesis highlights additional translational opportunities. In this context, the recent clinical success of PI3Kδ inhibitors for the treatment of mature B-cell malignancies is particularly noteworthy[48], for our data suggest that antiangiogenesis may be another putative mechanism for the clinical activity of these agents.

Recently, the contrast between abolishing blood supply versus normalizing tumor vasculature has come to the forefront in the angiogenesis field. The former, which derives from intensive and continuous use of agents that directly target VEGF and its receptors, creates a hypoxic environment that may result in the emergence of aggressive tumor sub-populations resistant to treatment and with heightened metastatic potential[1, 2]. Conversely, maneuvers that aim to restore tumor vasculature, primarily by deliberately using a less-intensive administration of anti-VEGF signaling agents, appear to actually establish a microenvironment that improves the efficacy of chemo, radio and immunotherapy[2]. We have

not yet directly probed whether PDE4 inhibition will result in destruction of blood vessels or a more nuanced normalization of tumor vasculature. However, as PDE4 inhibitors do not directly target VEGF signals on the endothelium, and instead impinge on the vasculature by primarily acting on the lymphoma cells, we suggest that this maneuver is more likely to mimic the low dose approach of anti-VEGF/R therapy, which appears to primarily increase blood perfusion[1, 2]. Paradoxically, the significant but not overwhelming decrease in microvessel density that we detected in mice treated with Roflumilast may represent this concept, especially because this was accompanied by a marked decrease in tumor burden and improved survival.

In summary, we identified a novel cross-talk between lymphoma cells and the microenvironment that influences angiogenesis. These data highlighted an unexpected role for the ubiquitous second messenger cAMP in controlling tumor angiogenesis, and uncovered unique opportunities for therapeutic intervention in this setting with the use of PDE4 inhibitors. The discovery of PI3K and AKT as mediators of cAMP-PDE4B effects towards VEGF expands the panel of actionable targets that may have antiangiogenic activities in DLBCL. Considering its model of action, there is a possibility that PDE4 inhibition instead of promoting blood vessel destruction would rather induce normalization of tumor vasculature, and hence yield better clinical outcomes than traditional anti-VEGF strategies.

Supplementary Material

Refer to Web version on PubMed Central for supplementary material.

Acknowledgements

We thank the Cancer Therapy and Research Center at UTHSCSA Core Pathology Tissue Bank for procurement of the primary DLBCL samples. We acknowledge Patricia Dahia for insightful suggestions during the execution of this project. This work was supported by CPRIT awards RP110200 and RP150277 (to R.C.T.A.) and a Cancer Center support grant P30 CA054174.

References

1. Welti J, Loges S, Dimmeler S, Carmeliet P. Recent molecular discoveries in angiogenesis and antiangiogenic therapies in cancer. J Clin Invest. Aug; 2013 123(8):3190–3200. [PubMed: 23908119]
2. Jain RK. Antiangiogenesis strategies revisited: from starving tumors to alleviating hypoxia. Cancer Cell. Nov 10; 2014 26(5):605–622. [PubMed: 25517747]
3. Sehn LH, Gascoyne RD. Diffuse large B-cell lymphoma: optimizing outcome in the context of clinical and biologic heterogeneity. Blood. Jan 1; 2015 125(1):22–32. [PubMed: 25499448]
4. Alizadeh AA, Eisen MB, Davis RE, Ma C, Lossos IS, Rosenwald A, et al. Distinct types of diffuse large B-cell lymphoma identified by gene expression profiling. Nature. Feb 3; 2000 403(6769):503–511. [PubMed: 10676951]
5. Lenz G, Wright G, Dave SS, Xiao W, Powell J, Zhao H, et al. Stromal gene signatures in large-B-cell lymphomas. N Engl J Med. Nov 27; 2008 359(22):2313–2323. [PubMed: 19038878]
6. Monti S, Savage KJ, Kutok JL, Feuerhake F, Kurtin P, Mihm M, et al. Molecular profiling of diffuse large B-cell lymphoma identifies robust subtypes including one characterized by host inflammatory response. Blood. Mar 1; 2005 105(5):1851–1861. [PubMed: 15550490]

7. Pasqualucci L. The genetic basis of diffuse large B-cell lymphoma. Curr Opin Hematol. Jul; 2013 20(4):336–344. [PubMed: 23673341]
8. Weinstock DM, Dalla-Favera R, Gascoyne RD, Leonard JP, Levy R, Lossos IS, et al. A roadmap for discovery and translation in lymphoma. Blood. Mar 26; 2015 125(13):2175–2177. [PubMed: 25814490]
9. Salven P, Orpana A, Teerenhovi L, Joensuu H. Simultaneous elevation in the serum concentrations of the angiogenic growth factors VEGF and bFGF is an independent predictor of poor prognosis in non-Hodgkin lymphoma: a single-institution study of 200 patients. Blood. Dec 1; 2000 96(12): 3712–3718. [PubMed: 11090051]
10. Gratzinger D, Zhao S, Tibshirani RJ, Hsi ED, Hans CP, Pohlman B, et al. Prognostic significance of VEGF, VEGF receptors, and microvessel density in diffuse large B cell lymphoma treated with anthracycline-based chemotherapy. Laboratory investigation; a journal of technical methods and pathology. Jan; 2008 88(1):38–47.
11. Cardesa-Salzmann TM, Colomo L, Gutierrez G, Chan WC, Weisenburger D, Climent F, et al. High microvessel density determines a poor outcome in patients with diffuse large B-cell lymphoma treated with rituximab plus chemotherapy. Haematologica. Jul; 2011 96(7):996–1001. [PubMed: 21546504]
12. Liapis K, Clear A, Owen A, Coutinho R, Greaves P, Lee AM, et al. The microenvironment of AIDS-related diffuse large B-cell lymphoma provides insight into the pathophysiology and indicates possible therapeutic strategies. Blood. Jul 18; 2013 122(3):424–433. [PubMed: 23652804]
13. Seymour JF, Pfreundschuh M, Trneny M, Sehn LH, Catalano J, Csinady E, et al. R-CHOP with or without bevacizumab in patients with previously untreated diffuse large B-cell lymphoma: final MAIN study outcomes. Haematologica. Aug; 2014 99(8):1343–1349. [PubMed: 24895339]
14. Stopeck AT, Unger JM, Rimsza LM, LeBlanc M, Farnsworth B, Iannone M, et al. A phase 2 trial of standard-dose cyclophosphamide, doxorubicin, vincristine, prednisone (CHOP) and rituximab plus bevacizumab for patients with newly diagnosed diffuse large B-cell non-Hodgkin lymphoma: SWOG 0515. Blood. Aug 9; 2012 120(6):1210–1217. [PubMed: 22734071]
15. Mosenden R, Tasken K. Cyclic AMP-mediated immune regulation--overview of mechanisms of action in T cells. Cell Signal. Jun; 2011 23(6):1009–1016. [PubMed: 21130867]
16. Levy FO, Rasmussen AM, Tasken K, Skalhegg BS, Huitfeldt HS, Funderud S, et al. Cyclic AMP-dependent protein kinase (cAK) in human B cells: co-localization of type I cAK (RI alpha 2 C2) with the antigen receptor during anti-immunoglobulin-induced B cell activation. Eur J Immunol. Jun; 1996 26(6):1290–1296. [PubMed: 8647207]
17. Kim SW, Rai D, McKeller MR, Aguiar RC. Rational combined targeting of phosphodiesterase 4B and SYK in DLBCL. Blood. Jun 11; 2009 113(24):6153–6160. [PubMed: 19369227]
18. Smith PG, Wang F, Wilkinson KN, Savage KJ, Klein U, Neuberg DS, et al. The phosphodiesterase PDE4B limits cAMP-associated PI3K/AKT-dependent apoptosis in diffuse large B-cell lymphoma. Blood. Jan 1; 2005 105(1):308–316. [PubMed: 15331441]
19. Serezani CH, Ballinger MN, Aronoff DM, Peters-Golden M. Cyclic AMP: master regulator of innate immune cell function. Am J Respir Cell Mol Biol. Aug; 2008 39(2):127–132. [PubMed: 18323530]
20. Conti M, Richter W, Mehats C, Livera G, Park JY, Jin C. Cyclic AMP-specific PDE4 phosphodiesterases as critical components of cyclic AMP signaling. J Biol Chem. Feb 21; 2003 278(8):5493–5496. [PubMed: 12493749]
21. Shipp MA, Ross KN, Tamayo P, Weng AP, Kutok JL, Aguiar RC, et al. Diffuse large B-cell lymphoma outcome prediction by gene-expression profiling and supervised machine learning. Nat Med. Jan; 2002 8(1):68–74. [PubMed: 11786909]
22. Kim SW, Rai D, Aguiar RC. Gene set enrichment analysis unveils the mechanism for the phosphodiesterase 4B control of glucocorticoid response in B-cell lymphoma. Clinical cancer research : an official journal of the American Association for Cancer Research. Nov 1; 2011 17(21):6723–6732. [PubMed: 21742807]

23. Mendes JB, Rocha MA, Araujo FA, Moura SA, Ferreira MA, Andrade SP. Differential effects of rolipram on chronic subcutaneous inflammatory angiogenesis and on peritoneal adhesion in mice. Microvascular research. Dec; 2009 78(3):265–271. [PubMed: 19732781]
24. Favot L, Keravis T, Holl V, Le Bec A, Lugnier C. VEGF-induced HUVEC migration and proliferation are decreased by PDE2 and PDE4 inhibitors. Thromb Haemost. Aug; 2003 90(2): 334–343. [PubMed: 12888882]
25. Jin H, Garmy-Susini B, Avraamides CJ, Stoletov K, Klemke RL, Varner JA. A PKA-Csk-pp60Src signaling pathway regulates the switch between endothelial cell invasion and cell-cell adhesion during vascular sprouting. Blood. Dec 16; 2010 116(25):5773–5783. [PubMed: 20826718]
26. Kim S, Bakre M, Yin H, Varner JA. Inhibition of endothelial cell survival and angiogenesis by protein kinase A. J Clin Invest. Oct; 2002 110(7):933–941. [PubMed: 12370271]
27. Lin AP, Abbas S, Kim SW, Ortega M, Bouamar H, Escobedo Y, et al. D2HGDH regulates alpha-ketoglutarate levels and dioxygenase function by modulating IDH2. Nature communications. 2015; 6:7768.
28. Jin SL, Conti M. Induction of the cyclic nucleotide phosphodiesterase PDE4B is essential for LPS-activated TNF-alpha responses. Proc Natl Acad Sci U S A. May 28; 2002 99(11):7628–7633. [PubMed: 12032334]
29. Jung I, Aguiar RC. MicroRNA-155 expression and outcome in diffuse large B-cell lymphoma. Br J Haematol. Jan; 2009 144(1):138–140. [PubMed: 19016736]
30. Bouamar H, Jiang D, Wang L, Lin AP, Ortega M, Aguiar RC. MicroRNA 155 Control of p53 Activity Is Context Dependent and Mediated by Aicda and Socs1. Mol Cell Biol. Apr 15; 2015 35(8):1329–1340. [PubMed: 25645925]
31. Mizukami Y, Kohgo Y, Chung DC. Hypoxia inducible factor-1 independent pathways in tumor angiogenesis. Clin Cancer Res. Oct 1; 2007 13(19):5670–5674. [PubMed: 17908955]
32. Kotani A, Kakazu N, Tsuruyama T, Okazaki IM, Muramatsu M, Kinoshita K, et al. Activation-induced cytidine deaminase (AID) promotes B cell lymphomagenesis in Emu-cmyc transgenic mice. Proc Natl Acad Sci U S A. Jan 30; 2007 104(5):1616–1620. [PubMed: 17251349]
33. Schuster C, Berger A, Hoelzl MA, Putz EM, Frenzel A, Simma O, et al. The cooperating mutation or “second hit” determines the immunologic visibility toward MYC-induced murine lymphomas. Blood. Oct 27; 2011 118(17):4635–4645. [PubMed: 21878673]
34. Hemann MT, Bric A, Teruya-Feldstein J, Herbst A, Nilsson JA, Cordon-Cardo C, et al. Evasion of the p53 tumour surveillance network by tumour-derived MYC mutants. Nature. Aug 11; 2005 436(7052):807–811. [PubMed: 16094360]
35. Schmitt CA, Rosenthal CT, Lowe SW. Genetic analysis of chemoresistance in primary murine lymphomas. Nat Med. Sep; 2000 6(9):1029–1035. [PubMed: 10973324]
36. Wendel HG, De Stanchina E, Fridman JS, Malina A, Ray S, Kogan S, et al. Survival signalling by Akt and eIF4E in oncogenesis and cancer therapy. Nature. Mar 18; 2004 428(6980):332–337. [PubMed: 15029198]
37. Nilsson JA, Keller UB, Baudino TA, Yang C, Norton S, Old JA, et al. Targeting ornithine decarboxylase in Myc-induced lymphomagenesis prevents tumor formation. Cancer Cell. May; 2005 7(5):433–444. [PubMed: 15894264]
38. Wall M, Poortinga G, Stanley KL, Lindemann RK, Bots M, Chan CJ, et al. The mTORC1 inhibitor everolimus prevents and treats Emu-Myc lymphoma by restoring oncogene-induced senescence. Cancer discovery. Jan; 2013 3(1):82–95. [PubMed: 23242809]
39. Bouamar H, Abbas S, Lin AP, Wang L, Jiang D, Holder KN, et al. A capture-sequencing strategy identifies IRF8, EBF1, and APRIL as novel IGH fusion partners in B-cell lymphoma. Blood. Aug 1; 2013 122(5):726–733. [PubMed: 23775715]
40. Li C, Kim SW, Rai D, Bolla AR, Adhvaryu S, Kinney MC, et al. Copy number abnormalities, MYC activity, and the genetic fingerprint of normal B cells mechanistically define the microRNA profile of diffuse large B-cell lymphoma. Blood. Jun 25; 2009 113(26):6681–6690. [PubMed: 19278952]
41. Gratzinger D, Zhao S, Marinelli RJ, Kapp AV, Tibshirani RJ, Hammer AS, et al. Microvessel density and expression of vascular endothelial growth factor and its receptors in diffuse large B-

cell lymphoma subtypes. The American journal of pathology. Apr; 2007 170(4):1362–1369. [PubMed: 17392174]

42. Norrby K, Ridell B. Tumour-type-specific capillary endothelial cell stainability in malignant B-cell lymphomas using antibodies against CD31, CD34 and Factor VIII. APMIS : acta pathologica, microbiologica, et immunologica Scandinavica. Apr; 2003 111(4):483–489.
43. Gantner F, Gotz C, Gekeler V, Schudt C, Wendel A, Hatzelmann A. Phosphodiesterase profile of human B lymphocytes from normal and atopic donors and the effects of PDE inhibition on B cell proliferation. Br J Pharmacol. Mar; 1998 123(6):1031–1038. [PubMed: 9559883]
44. Tsunoda T, Ota T, Fujimoto T, Doi K, Tanaka Y, Yoshida Y, et al. Inhibition of phosphodiesterase-4 (PDE4) activity triggers luminal apoptosis and AKT dephosphorylation in a 3-D colonic-crypt model. Molecular cancer. 2012; 11:46. [PubMed: 22830422]
45. Sengupta R, Sun T, Warrington NM, Rubin JB. Treating brain tumors with PDE4 inhibitors. Trends Pharmacol Sci. Jun; 2011 32(6):337–344. [PubMed: 21450351]
46. Wang P, Wu P, Ohleth KM, Egan RW, Billah MM. Phosphodiesterase 4B2 is the predominant phosphodiesterase species and undergoes differential regulation of gene expression in human monocytes and neutrophils. Mol Pharmacol. Jul; 1999 56(1):170–174. [PubMed: 10385698]
47. Pullamsetti SS, Banat GA, Schmall A, Szibor M, Pomagruk D, Hanze J, et al. Phosphodiesterase-4 promotes proliferation and angiogenesis of lung cancer by crosstalk with HIF. Oncogene. Feb 28; 2013 32(9):1121–1134. [PubMed: 22525277]
48. Yang Q, Modi P, Newcomb T, Queva C, Gandhi V. Idelalisib: First-in-Class PI3K Delta Inhibitor for the Treatment of Chronic Lymphocytic Leukemia, Small Lymphocytic Leukemia, and Follicular Lymphoma. Clin Cancer Res. Apr 1; 2015 21(7):1537–1542. [PubMed: 25670221]

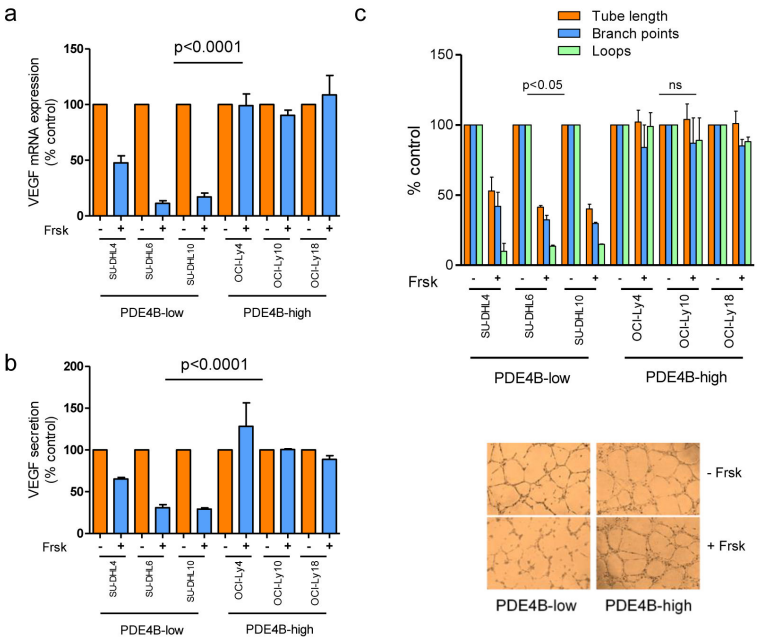

Figure 1. Cyclic-AMP-mediated PDE4B-dependent suppression of VEGFA in DLBCL

a) Quantitative real-time RT-PCR shows that *VEGFA* mRNA levels are significantly reduced following increase in the intracellular levels of cAMP (10 μM Forskolin, Frsk, for 6hrs) exclusively in DLBCL cell lines expression low levels of PDE4B ($p<0.0001$, ANOVA; $p<0.05$ Bonferroni's multiple comparison post-test for PDE4B-low cell lines, non-significant for PDE4B-high cells). Data shown are the mean ± SD of an assay performed in triplicate. Three biological replicates were completed. In all instances, *VEGFA* expression was normalized to that of a housekeeping gene *TBP*, and relative quantification achieved by calculating ΔΔCt, and expression defined as $2^{-\Delta\Delta Ct}$, where cells exposed to vehicle represent the baseline. **b)** VEGF quantification in the supernatant of DLBCL cell lines assay shows a significant cAMP-mediated suppression in DLBCL cell lines expressing low PDE4B but not in those with high levels of this enzyme ($p<0.0001$, ANOVA; $p<0.05$ Bonferroni's multiple comparison post-test for PDE4B-low cell lines, non-significant for PDE4B-high cells). Data shown are the mean ± SD of three independent biological replicates**. c)** Top - relative quantification of three output measures (tube length, branch point and loops) for the HUVEC tube formation assay is shown. Conditioned media from PDE4B-low DLBCL cell lines exposed to Forskolin were significantly less efficient in promoting tube formation, while no changes were detectable in DLBCL cell lines expressing high PDE4B ($p<0.05$, two-tailed Student's t-test for each measure in PDE4B-low cell lines; non-significant in the PDE4B-high).. Data shown are the mean ± SD of two independent biological replicates, each performed in triplicate. Note that the conditioned media used in b) and c) do not contain Forskolin, this drug was washed-off from the culture 24h before supernatant collection.

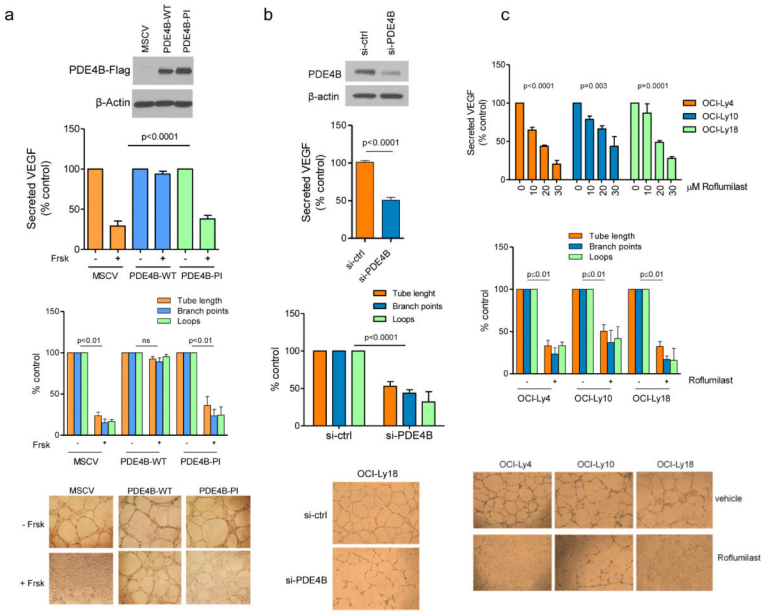

Figure 2. Genetic and pharmacological modulation of PDE4B in DLBCL regulates VEGF levels and HUVEC tube formation

a) Top - VEGF quantification in the supernatant of the PDE4B-low SU-DHL6 cell line expressing an empty vector (MSCV), wild-type PDE4B (WT) or a phosphodiesterase inactive (PI) mutant. PDE4B-WT abolished Forskolin (cAMP) effects on VEGF ($p<0.0001$, ANOVA; $p<0.05$ Bonferroni's multiple comparison post-test for MSCV and PDE4B-PI and non-significant for PDE4B-WT). Data shown are the mean ± SD of four biological replicates. Expression of PDE4B was confirmed by WB. Concordantly, conditioned media from Forskolin-exposed PDE4B-WT cells did not impair the tube-forming capacity of HUVEC (bottom graph). Data shown are the mean ± SD of three biological replicates ($p<0.01$, two-tailed Student's t-test for each measure in MSCV and PDE4B-PI CELLS; non-significant for PDE4B-WT). Tube formation images are shown below the graph. **b)** Top - VEGF quantification in the supernatant of the PDE4B-high cell line OCI-Ly18 transfected with PDE4B-specific siRNA oligonucleotides. Knockdown (KD) of PDE4B (confirmed by WB) decreased VEGF secretion ($p<0.0001$, two-tailed Student's t-test, si-ctrl vs. si-PDE4B). Conditioned media from Forskolin-exposed PDE4B-KD cells impaired tube-forming capacity of HUVEC (bottom graph) ($p<0.001$, two-tailed Student's t-test, for each tube formation measure). Data shown are mean ± SD of six data point derived from two biological replicates. Tube formation images are at the bottom. **c)** Top - VEGF quantification in the supernatant of the PDE4B-high DLBCL cell lines exposed to vehicle or Roflumilast. PDE4 inhibition suppressed VEGF secretion in all models analyzed ($p<0.01$ ANOVA for all cell lines; $p<0.05$ Bonferroni's multiple comparison post-test). Data represent the mean ± SEM of three biological replicates. Concordantly, conditioned media from Roflumilast-treated cell lines (30 μM) impaired the tube formation capacity of HUVEC ($p\leq0.01$ two-tailed Student's t-test for each measure in each cell line) (bottom graph). Data shown are mean ± SD of an assay performed in triplicate; two biological replicates were completed. Representative tube formation images are shown at the bottom. The conditioned media used

in these assays do not contain Forskolin or Roflumilast, these agents were washed-off and the cells cultured in drug-free media for 24h before collection.

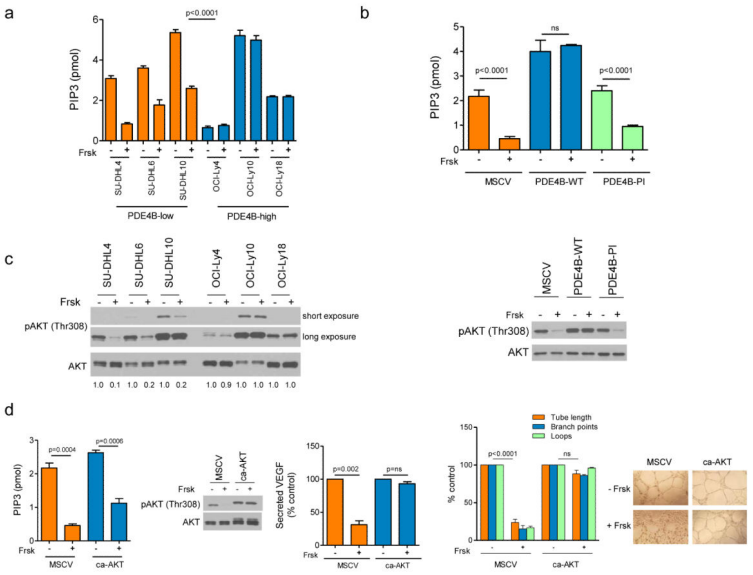

Figure 3. The cAMP/PDE4B axis influences VEGF expression by modulating PI3K/AKT signals

a) Elevation of the intra-cellular levels of cAMP with Forskolin (Frsk) significantly suppressed PI3K activity (represented by the amount of PIP3 generated) in DLBCL cell lines expressing low PDE4B levels, but it had no effect in PDE4B-high cell lines (<0.0001, ANOVA; p<0.0001 Bonferroni's multiple comparison post-test for PDE4B-low and non-significant for PDE4B-high cell lines). In this assay, all lysates were collected following BCR activation with goat anti-human IgM/IgG (10μg/ml for 10 minutes) **b)** Stable expression of PDE4B-WT, but not of an inactive mutant or empty-vector abrogated the ability of cAMP to suppress PI3K activity in the isogenic SU-DHL6 models (p<0.0001, ANOVA; p<0.0001 Bonferroni's multiple comparison post-test for MSCV and PDE4B-PI and non-significant for PDE4B-WT). Data in a) and b) are mean ± SD of assays performed in triplicate. The data were validated with two biological replicates. **c)** Western blot analysis of BCR-activated DLBCL cell lines shows that Forskolin exposure suppressed AKT phosphorylation (T308) in PD4B-low but not PDE4B-high cells (left panel). Ectopic expression of a functional PDE4B gene (WT), but not of an inactive mutant or empty-vector, in PDE4B-low SU-DHL6 cell line abolished cAMP (Frsk) effects towards AKT phosphorylation (right panel). **d)** Stable expression of constitutive active (ca) AKT did not alter the effects of cAMP (Frsk) towards PI3K (left panel) but it blocked the effects of this second messenger on AKT phosphorylation (T308), VEGF secretion (middle graph) and HUVEC tube formation (right side graph). Representative tube formation images are shown at the bottom. Note that the conditioned media used in these assays do not contain Forskolin, this drug was washed-off from the culture 24h before supernatant collection. The PIP3 data are mean ± SD of an assay performed in triplicate (p values are two-tailed Student's t-test). The data were validated with two biological replicates. The VEGF secretion and tube formation assays are mean ± SD of three independent biological replicates (p values are two-tailed Student's t-test for each measure in each cell model).

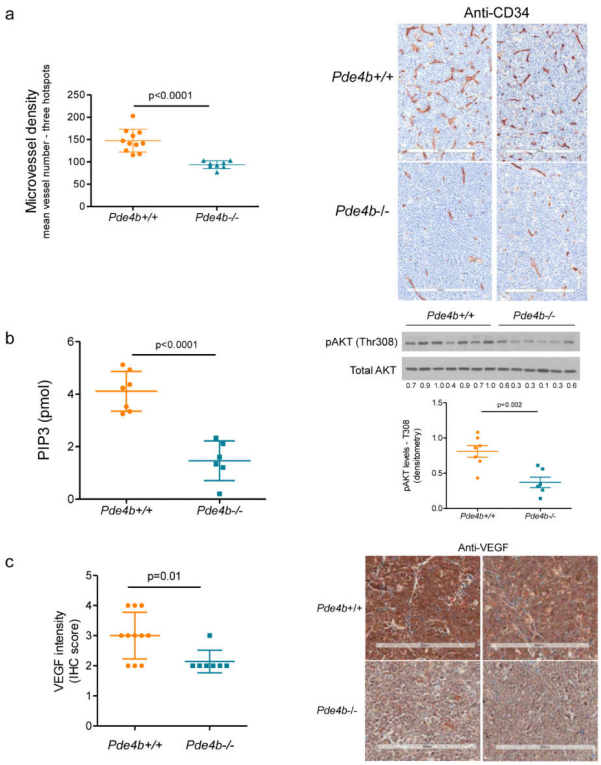

Figure 4. Genetic ablation of *PDE4B* limits angiogenesis in vivo

a) Microvessel density (MVD) of B-cell lymphomas derived from *Pde4b+/+* and *Pde4b−/−* mice was assayed by CD34 immunohistochemistry and shown to be significantly reduced in the *Pde4b* deficient mice (p<0.0001, two-tailed Student's t-test). Data shown are mean vessel number from three hot-spots ± SD; each dot in the graph represents a unique tumor (n=19). Representative CD34 IHC of murine B-cell lymphomas are shown in the right panel. The size bar indicates 200 μm. **b)** Lymphomas arising in *Pde4b−/−* show significantly lower PI3K activity (left panel) and AKT phosphorylation (T308, quantified by densitometry, right panel) (p<0.0001 and p=0.002, respectively, two-tailed Student's t-test). Data shown are mean ± SD of an assay performed in triplicate (n=13; 7 *Pde4b+/+* and 6 *Pde4b−/−* lymphomas). **c)** Lymphomas from *Pde4b−/−* mice show significantly lower VEGF abundance than tumors arising in *Pde4b+/+* mice (p=0.01, two-tailed Student's t-test). Data shown are mean ± SD of IHC scores (n = 18; 11 *Pde4b+/+* and 7 *Pde4b−/−* lymphomas). Representative VEGF IHC of murine B-cell lymphomas are shown in the right panel. The size bar indicates 200 μm.

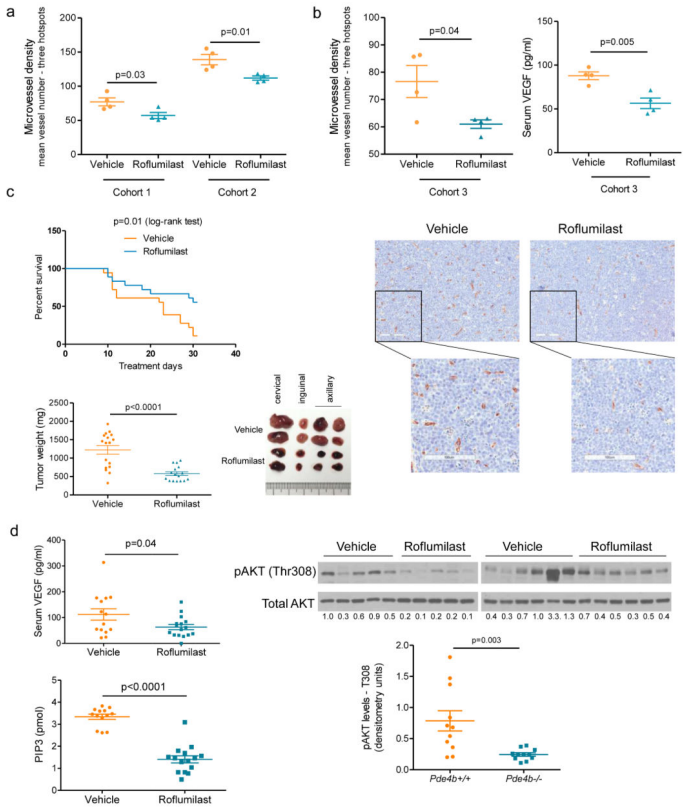

Figure 5. Pharmacological targeting of Pde4 limits angiogenesis and improves survival in a murine model of B-cell lymphoma

a) MVD of B-cell lymphomas from two independent cohorts of mice (n=16) randomized to receive Roflumilast or vehicle control show a significantly suppressed angiogenesis in mice treated with the PDE4 inhibitor (p=0.03 and p=0.01, cohorts 1 and 2 respectively, two-tailed Student's t-test). Data shown are mean vessel number from three hot-spots ± SEM; each dot in the graph represents a unique tumor **b)** MVD of B-cell lymphomas from a third independent cohort of mice (n=8) randomized to receive Roflumilast or vehicle control show a significantly suppressed angiogenesis in mice treated with the PDE4 inhibitor in association with diminished serum levels of VEGFA (p=0.04 and p=0.005 left and right graphs, respectively, two-tailed Student's t-test). Data shown are mean vessel number from three hot-spots or VEGF quantification ± SEM; each dot in the graph represents a unique tumor. Representative CD34 IHC of murine B-cell lymphomas are shown in the bottom panel. The bar indicates 100μm **c)** Top graph - Kaplan-Meier survival curves of mice bearing isogenic *Eu-myc* lymphomas treated with vehicle or Roflumilast. The log-rank test showed a significantly improved survival rate in the Roflumilast-treated mice (n=36, p=0.01). Bottom graph – lymphomas excised from Roflumilast-treated mice were significantly smaller than those derived from mice treated with a vehicle control (p<0.0001, two-tailed Student's t-test, n=33). Representative examples of lymphomas collected from these mice are shown on the right. **d)** Circulating levels of VEGFA and tumoral PI3K activity (top and bottom graphs, respectively) were significantly lower in mice randomized to receive Roflumilast than in vehicle control treated mice (p=0.04 and p<0.0001, respectively, two sided Student's t-test). Data shown are mean ± SEM of 30 mice and 28 tumors, respectively; PIP3 levels were

measured in triplicates. Right panel - western blot examination of primary murine B-cell lymphomas indicate that AKT phosphorylation (T308) is significantly suppressed following Roflumilast administration (p=0.003, two-tailed Student's t-test – densitometric pAKT values, normalized by totaL AKT, n=22).

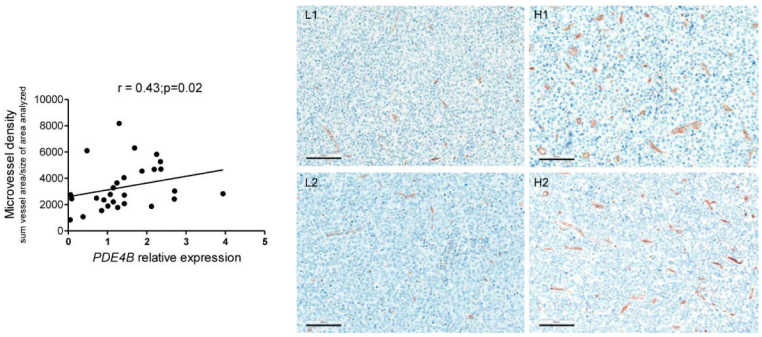

Figure 6. Correlation between PDE4B expression and angiogenesis in primary human DLBCL

Linear regression analysis between *PDE4B* expression quantified by real-time RT-PCR and microvessel density, determined by CD34 staining, in 28 primary human DLBCLs (Spearman's correlation coefficient r=0.43, p=0.02). Representative CD34 staining of DLBCLs with low or high MVD (left and right, respectively) is also shown. The size bar indicates 100 μm.